Final Technical Report
for
Office of Naval Research
Award Number N000140410016

Scientific Officers: Dr. E. S. Livingston, Dr. D. B. Reedcr

Shallow Water Propagation

Principal Investigator: Dr. William L. Siegmann
Rensselaer Polytechnic Institute
110 Eighth Street
Jonsson-Rowland Science Center 1C08
Troy, New York 12180-3590
phone: (518) 276-6905 fax: (518) 276-2825 email: siegmw@rpi.cdu

I. SUMMARY

This is the Final Technical Report for ONR Award Number N000140410016, which commenced on 1 October 2003, was renewed on 1 October 2006, and terminated on 30 September 2009. During the performancc period, six students received their PhD degrecs from Rensselaer Polytechnic Institute with ONR support, and their initial and current positions are provided in Section IV. Twenty-one papers were published, including ten in the *Journal of the Acoustical Society of America* and six in *IEEE* publications, and their references are listed in Section V. Thirty-six professional presentations were made, including thirty-two at national or international meetings, and their titles and venues are given in Section VI. Some research results and figures from the performance period are highlighted in Sections II and III.

II. RESEARCH HIGHLIGHTS

A. Propagation Model Development and Applications

- Layered elastic sediments are important in shallow water and must be accurately handled as the basis for extensions to more complicated bottoms that include range dependence, poro-elasticity, and other physical mechanisms. Our parabolic equation formulation [1] resolved this task by using new choices of dependent variables, along with the same efficient and reliable numerical schemes as for fluid bottom models. The formulation accommodates all physical conditions at layer interfaces and avoids stability difficulties that arise in other approaches. ***Figure 1*** illustrates results from our implementation. Comparing the upper and middle contour plots, we conclude that significant transmission level differences can occur in the ocean as a result of the elastic bottom waveguide. The lower contour plot demonstrates that this method, unlikc other parabolic equations, can treat seismic sources.

- Shallow-water propagation problems may involve acoustic energy interactions between the ocean, different types of sediments, and other features such as beaches and sandbars. Our parabolic equation formulation for elastic sediments allows regions with small slope changes to be handled accurately and efficiently. An extension using a mapping approach [2] applies to shallow-water environments with complex layering and steep slopes, requiring only that the rate of slope changes is sufficiently gradual. Acoustic energy exchanges that result from range evolution of interfaces can have significant impacts on propagation characteristics. An illustration is the transmission-loss contour plot in ***Figure 2***, showing an ocean over an elastic sediment which is above an elastic basement and for which the water-sediment bathymetry rises to the surface to form a beach. A Scholte wave develops near the bathymetric interface and propagates up the slope to the start of the beach, where the wave energy transitions into a Rayleigh wave near the air-sediment boundary. A significant portion of the energy in this low-frequency example persists as it propagates inside the sediment layer and up the beach. We conclude that our method has capabilities for investigating propagation interactions, including wave conversion mechanisms, between the ocean and sediment layers.

- One challenge for shallow-water propagation predictions is accurate treatment of acoustic interaction with layered elastic sediments in which the layer interfaces as well as the bathymetry are range dependent. When sediment morphology data is available, interface range variations are invariably observed. Our parabolic equation formulation for range-independent layered elastic sediments satisfies all physical conditions at interfaces while maintaining robust computational stability. This method has been extended [8] to treat certain types of range-dependent interfaces, which can have important effects on propagation characteristics. The upper contour plot in ***Figure 3*** illustrates a three-layer sediment having a dome formation in the lowest layer that blocks propagation in the middle layer, which regains some of the acoustic energy beyond the dome. The lower contour plot shows a two-layer sediment with a strong density contrast that permits a Stoneley wave to propagate along the undulating interface. We conclude from these and other examples that our method provides unique capabilities for determining geoacoustic influences on shallow-water predictions.

- Range dependence at an ocean-elastic boundary is a very important environmental feature in shallow water, because shelves, beaches, and different sediment morphology produce dramatic interface variations. A mapping technique and our elastic parabolic equation formulation handle environments with complex layering and steep slopes, so long as the rates of slope changes are sufficiently gradual. Another result [3] uses an entirely different coordinate rotation method that not only allows larger slope rates but also increases accuracy by removing an approximation necessary in the mapping approach. Frequent range changes of the ocean-elastic bathymetric interface and of the underlying sediment heterogeneity present no difficulties for determining the evolution of acoustic energy. One example is the loss contours in ***Figure 4***, for an ocean above two distinct elastic sediment layers over an elastic basement, with the interfaces varying on scales of one to five wavelengths. Strong waveguide propagation occurs in both sediment layers as well as the ocean, along with some energy exchange between layers. A Scholte wave is generated near the bathymetry and persists along the entire range-dependent interface. We conclude that our method provides unmatched capabilities for accurately handling relatively rapid range dependence, along with energy exchange between wave types and with other propagation phenomena.

- Shallow water propagation problems require full capabilities for propagation over and through range-dependent elastic sediments. The two primary difficulties are accurate treatments of ocean-sediment/air-sediment boundary variations and of elastic-elastic interfaces in the sediment. A general capability is essential, since complex sediment morphology can produce strong interface variations that dramatically affect propagation. Our approach relies on a combination of single scattering at vertical elastic-elastic interfaces and a powerful iteration procedure [4] that assures convergence for interface slopes and elastic property changes which are as large as needed for applications. Substantial changes in the stratigraphy of sediment heterogeneities present no difficulties in determining the evolution of acoustic energy. One example is shown by the loss contours in ***Figure 5,*** for a four-layer elastic medium with interfacial range dependence so strong that one of the layers disappears at one range and returns at a longer range. Waveguide propagation is visible in two of the layers, along with energy exchanges among the upper layers. We conclude that our method provides unparalleled capabilities for accurately handling elastic environments with significant range dependence.

- Ocean acoustic data analysis and applications require accurate and efficient calculation of propagation in shallow water waveguides including range dependent elastic sediments. The solutions of such problems are necessary to evaluate mechanisms of shear energy generation and propagation. Our parabolic equation procedure [5] has evolved from a series of advances: a formulation using non-traditional dependent variables; a technique using coordinate rotations at ranges where changes in bathymetry slope occur; single scattering corrections at stair-step approximations of sediment interfaces and elastic parameter variations; and an efficient iteration procedure for realistically large elastic parameter and slope changes. The capabilities of the method for shallow water problems are illustrated in ***Figure 6***. The upper panel illustrates complicated stratigraphy and sediment structure at the New Jersey coastal AGS site on one acoustic track, along which a University of Delaware experiment was conducted and detailed core profiling was available. The middle panel shows 50 Hz transmission loss contours for the sediment modeled by just two homogeneous layers. The bottom panel contours are obtained for the sediment modeled by eight homogeneous layers and stratigraphy constructed to correspond closely to the upper panel. The acoustic energy patterns in the two contour figures differ sharply, both in the sediments and in the water. We conclude from such results that our new propagation approach provides the necessary capabilities for efficient and accurate propagation calculations in shallow water waveguides with range variations in elastic sediment structure and layering.

- An essential capability for ocean acoustic data analysis and applications is accurate and efficient propagation calculations in shallow water waveguides that involve range dependent elastic sediments. Sediment elasticity is important because transferring energy between compressional and shear modes may significantly influence the overall intensity field. Effective treatment of elasticity is also the necessary precursor for handling poro-elastic and other complex sediments. The physical and computational challenge, which has delayed progress for decades, is that the spectral distribution of energy is much broader in wave number space than for fluid sediments. The capabilities of our method continue to expand, one example being the treatment of propagation into and up a sloping beach [7]. An environment motivated by the topography and stratigraphy on the Southern California coast is illustrated in ***Figure*** *7*. The upper panel shows compressional energy at 150 Hz propagating in both sediment layers, up the beach beyond 1.8 km, and with modal cutoff in the sediment. The influence of topography on the loss field arises from propagation into the beach, without which energy would be lost to modal cutoff. The middle panel shows very good agreement between results from the method and a full field finite-element calculation. The bottom panel shows inadequate agreement between results for the full field and the only other parabolic equation capable of handling beach propagation, because its validity limits are exceeded by the environmental variability here. We conclude from these and other results that our propagation method provides necessary capabilities for efficient and accurate calculations in shallow water waveguides with range variations in bathymetry, topography, and elastic sediment structure and layering.

B. <u>Environmental Features, Acoustic Effects, and Data Comparisons</u>

- Several multi-participant experiments have confirmed that large amplitude internal solitons, which occur in many shallow water environments, significantly affect acoustic variability. Their influence on broadband signals is a fundamental research issue whose resolution also has consequences for systems applications. In developing simulations for two tracks in the SWARM95 experiment, we found [11] that modeling the behavior of received signal-integrated energy can determine the quantitative effects of solitons. One illustration in ***Figure 8*** shows depth-averaged data at the Naval Research Laboratory vertical line array (VLA) [dashed blue curves] from a source 18 km away, compared with parabolic equation simulations [solid red] that account for a train of eight solitons. Both observations and computations show similar oscillations with time that arise from the propagating solitons, in filtered bands centered at 32 Hz [upper] and 64 Hz [middle], and over the full source spectrum [lower, plotted about mean energy]. The physical mechanism causing the variations is coupling between wave numbers from soliton energy spectrum peaks and from differences of dominant acoustic modes. We conclude that this mechanism, known previously to operate for cw sources and high frequencies, also occurs for broadband sources at low frequencies.

- Major field experiments demonstrate the important role of tidally generated and bathymetrically modified internal solitons in many shallow-water environments. In the SWARM95 experiment, the same broadband air gun signals were transmitted along one pair of experimental tracks. The critical distinction is that the tracks made different angles with the wave fronts of dominant internal solitons that were traversing them. Along one track we found that the source of observed variations in received signals was coupling between wave numbers from soliton spectral peaks and differences in principal acoustic modes. Along the other track, for which the aforementioned angle was small, thc variability was produced from energy focusing and dcfocusing that was caused by the soliton wave fronts [12]. An example is shown in ***Figure 9***, where thc left panel [black curves] displays filtered pulses observcd at one hydrophone on thc Woods Hole vertical line array about 15 km from the sourcc. The right panel [blue curves] compares corresponding simulations from a three-dimensional adiabatic modc parabolic equation, using an environmental containing a train of cight solitons. Both observations and computations show similar featurcs, in thc timc variability of pulse amplitude and second-mode arrival times, which arise from thc passagc of the solitons. We conclude that the mechanism of horizontal refraction produced by strong oceanic variability, which was studied by previous researchers but never previously documented in experimental data, can occur in shallow water and cause pulsc-integrated energy variations of about 6 dB.

- Since large-amplitude internal solitons can affect shallow-water acoustic variability substantially, it is important to quantify their influence for data analysis and predictions. For example, propagation in dircctions near those of soliton wave fronts, which are often roughly linear, can produce surprising features. Ducting occurs between solitons in a packet, and an intcrfcrence pattern analogous to Lloyd's Mirror arises at the leading cdge of the packct. From computations using a three-dimensional adiabatic mode parabolic equation and standard packet rcpresentations, we found that the "mirror" structure can producc typical intensity changes in the 6-10 dB range [14]. It is essential to determine if such changes persist when soliton properties are not specified exactly but have effectively random variations, as observations suggcst. Rcsults from one set of calculations are shown in ***Figure 10***, in which the upper panel is a schematic snapshot of a wave packet with diffcrent amplitudes and corresponding widths for each soliton. The bottom panel shows thc scintillation index for intensity variations, obtained by averaging over a set of packet realizations. Substantial fluctuations occur in the locations where, in the absence of randomness, low incident angle propagation produces the largest intensity variations. We conclude from the calculations that not only can soliton packets produce significant intensity changes, but also thcsc changes can pcrsist with random packct-propcrty variations of typical sizc.

- A fundamental issue for broadband propagation is thc typc and amount of environmental data that is required for useful estimates of quantitics such as averagcd transmission loss, signal gain, and coherence. Particularly important in shallow water are the robustness of predictions and critical parameter sensitivities. For the Strait of Korea we developed a geophysically based, four layer geoacoustic model using one set of transmission loss data from one Acoustic Characterization Tcst III experimental leg. Parabolic equation predictions, including parameterization of nonlinear frequency dependence in the upper scdimcnt layer attenuation, agree well with othcr data from thc same leg. Calculations using this model and available sound specd profiles and bathymetry were compared with independent broadband and narrowband data from a distinct but nearby leg of thc same experiment [15]. ***Figure 11*** shows the excellent agrcement obtained. Wc conclude that robust, site-specific environmental models are feasible for avcrage loss prcdictions if nonlinear frequcncy dcpendencc of sediment attenuation is included.

- Propagation predictability at low frequencies remains a critical problem in shallow water waveguides. Particular interest is in the relatively widespread regions with moderate range dependence and sandy-silty sediments. It is essential to quantify the connections between the intrinsic sediment attenuation and the overall decrease of transmission loss with range. When high quality measurements are available, propagation modeling can unravel the interactions, not only at the lowest frequencies where loss patterns can often be modeled in detail but also at frequencies with many propagating modes [17]. A useful metric is an effective attenuation coefficient (EAC) for the reduced transmission loss, determined by suitable range and depth averages of measurements and parabolic equation calculations. Results for 700 Hz from the 1993 ACT II experiment are displayed in the upper panels of ***Figure 12.*** The left panel shows reduced loss, with measurements in red and calculations in black. The right panel shows range-window-averaged loss and linear fits (with calculations displaced), the slopes of which are the EACs. Critical parameters for the calculations are the frequency-power exponent and near-bathymetry value of the upper layer sediment attenuation, along with the water sound speed and bathymetry profiles. The lower panel is a scatter plot of measured and calculated EACs for frequencies above 400 Hz in the Acoustic Characterization Test II and 1988 New Jersey Shelf experiments. The best fit line, which has slope one if the calculations exactly model the measurements, is sensitive to values of the critical parameters. Consistent with analyses for other sandy-silty locations, the attenuation frequency-power exponent and surface values are in the ranges [1.8, 2.0] and [0.33, 0.35] dB/m. We conclude that significant nonlinear frequency dependence of the upper sediment attenuation is necessary, and that few site-specific parameter values have major effects on the loss decrease at low frequencies.

- The intrinsic sediment attenuation in shallow water waveguides is a critical quantity for propagation predictability at low frequencies. A common situation is ocean environments with sandy-silty sediments, moderately small bathymetry variations, and typical water volume range dependence. The frequency behavior of the intrinsic attenuation is anticipated from Biot theory to have a power-law behavior with exponent 2. Results from several methods over many experimental sites suggest that the power-law exponent is consistently about 5 to 15% lower than 2. An explanation of the mechanism for this behavior has been formulated at Boston University. In a coordinated effort, we developed a procedure for estimating the power-law exponent and used it for extensive sensitivity investigations [16]. The most useful metric for the procedure was found to be the effective attenuation coefficient (EAC) for the reduced transmission loss. Because estimates of the key intrinsic attenuation parameters (the frequency power exponent and the near surface value) rely on EAC values, it is essential to examine the sensitivity of the metric to variations in water sound speed profiles, bathymetry, and other quantities. For example, ***Figure 13*** shows all measured water profiles for ACT II, along with a representative composite profile C (red) and the profile 64 (green) which is closest to the source location. As expected profile C provides very good comparisons between measured and calculated EACs, and profile 64 does nearly as well. A sample of six profiles from one run along one experimental track is shown in the middle panel. The EACs calculated using either all six of these profiles or their average profile S (blue) compare poorly with measurements. We conclude from these and related calculations that the selection of a representative water profile is important for estimates of sediment attenuation parameters, while moderate range dependence in profiles and bathymetry is not.

- One essential capability for ocean acoustics applications is propagation over and through range-dependent elastic sediments. Our parabolic equation method, with its unique formulation and extended capabilities, is an efficient procedure for a wide range of values for slopes and elastic parameters. Accuracy checks of this method for simple test problems show better results than standard procedures, such as approximating bathymetry slopes by stair steps and using a simplified energy-conservation condition at vertical interfaces. A critical question is propagation model performance in comparisons with experimental measurements. Strenuous tests are available using high quality measurements from laboratory experiment of propagation over an elastic slab in a large water tank at the Naval Research Laboratory [18]. Single-frequency propagation loss curves with the slab in a sloping configuration are shown as blue curves in ***Figure 14***. The upper panel shows that the green curve, from the new method using frequency/length scaling factor of 1000, provides a strikingly close comparison with data. The red curve, from a fluid-model bottom and displaced for clarity, has completely mismatched the pattern phase and amplitude behavior. The lower panel, for a frequency three times larger and many more propagating modes, shows remarkable agreement between the modal interference patterns. We conclude from these and related results that our propagation model provides a powerful and efficient tool for high accuracy calculations in range-dependent ocean seismo-acoustic waveguides.

III. FIGURES

A. Propagation Model Development and Applications

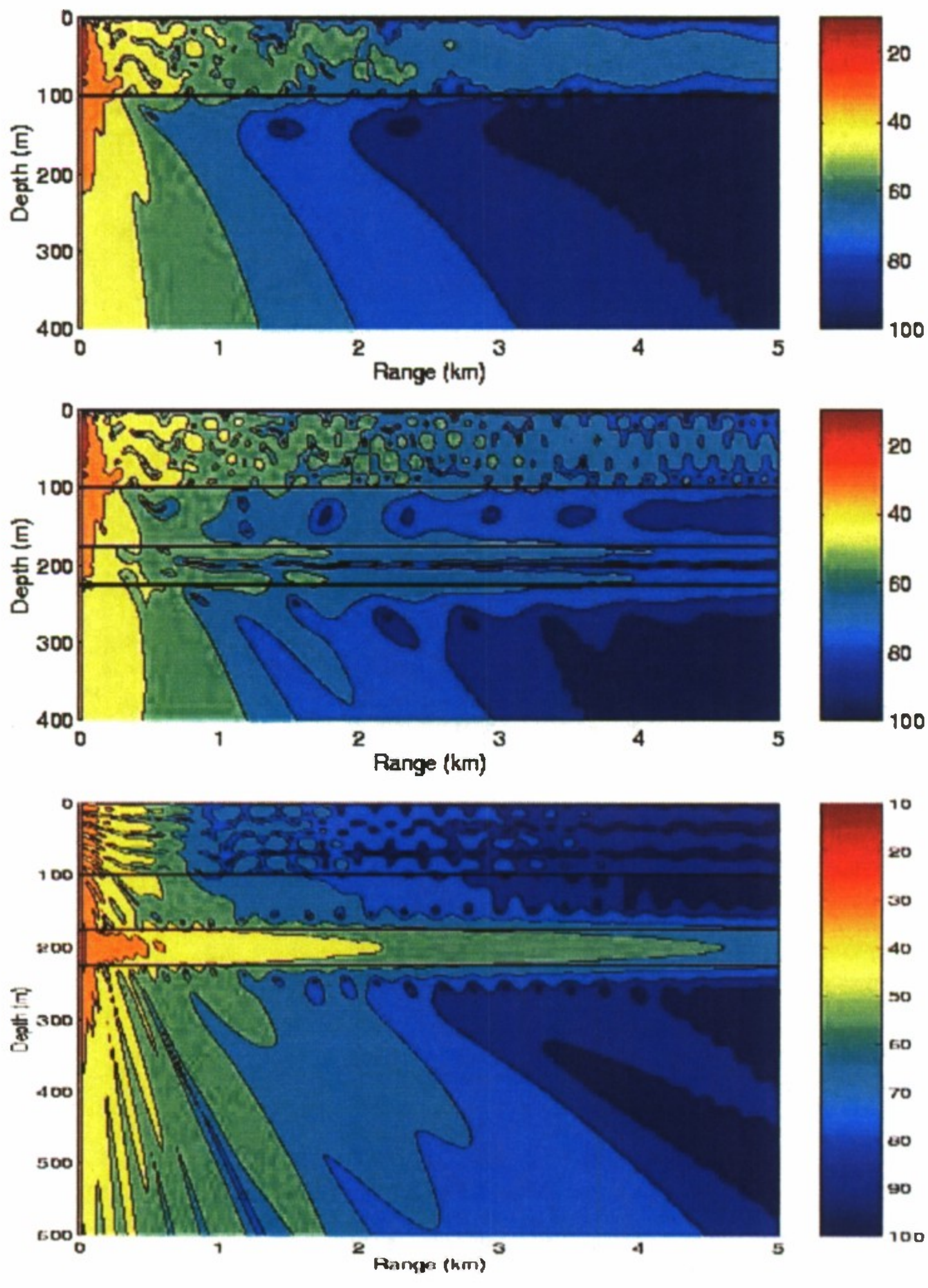

<u>Figure 1 (previous page)</u>. Ocean propagation can be affected by layered elastic sediments, which are treated accurately and efficiently by our parabolic equation formulation. Transmission loss contours (to 5 km range and at least 400 m depth) for source frequency 25 Hz are shown for a shallow ocean ($c_w = 1500$ m/s, $d = 100$ m) overlying an elastic sediment. <u>Upper:</u> Sediment is an elastic half space ($c_p = 1900$ m/s, $c_s = 900$ m/s, $\rho = 1.3$ gm/cm^3), and source depth $z_s = 10$ m. After 2.5 km the water column energy is mainly in the lowest mode. <u>Middle:</u> A low speed layer ($c_p = 1600$ m/s, $c_s = 700$ m/s) is sandwiched in the elastic half space between 175 and 225 m. Substantially higher energy (up to 20 dB) propagates in the elastic waveguide. Multiple modes still propagate in the water at 5 km. <u>Lower:</u> Same layered environment with $z_s = 200$ m. The new formulation applies for seismic sources, with energy strongly channeled into the elastic waveguide.

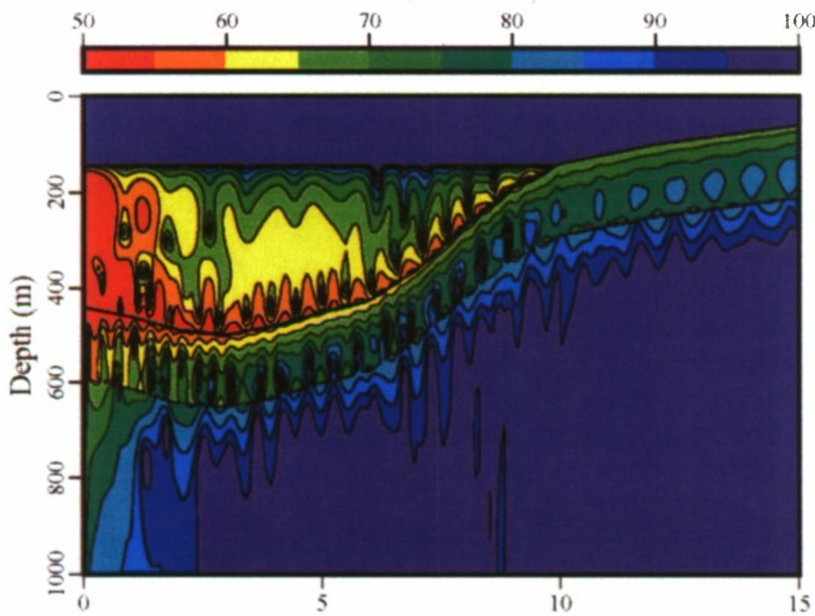

<u>Figure 2</u>. Many propagation problems involving range-dependent transitions between water and elastic sediments can be handled efficiently and accurately using a hybrid parabolic equation approach. Transmission loss contours, to 1000 m in depth and 15 km in range for a 5 Hz source, are shown for a beach environment. The ocean depth is 300 m at the initial range (where the source is 5 m above the bottom), then increases to a maximum of 360 m at about 3 km, and finally decreases with variable slope to zero at 10 km. An elastic sediment layer is 150 m thick and follows the bathymetry for the first 10 km, after which its upper surface forms a beach that rises with uniform slope to 80 m above sea level at 15 km. The sediment layer has compressional and shear sound speeds of 2400 and 1200 m/s, attenuations of 0.05 and 0.1 dB/λ, and density 1.5 gm/cm^3. The basement below the elastic layer has higher sound speeds and density. The contours illustrate a conversion between interfacial wave types. A Scholte wave develops at the water-sediment bathymetry, and the energy in this wave moves into a Rayleigh wave at the air-sediment boundary.

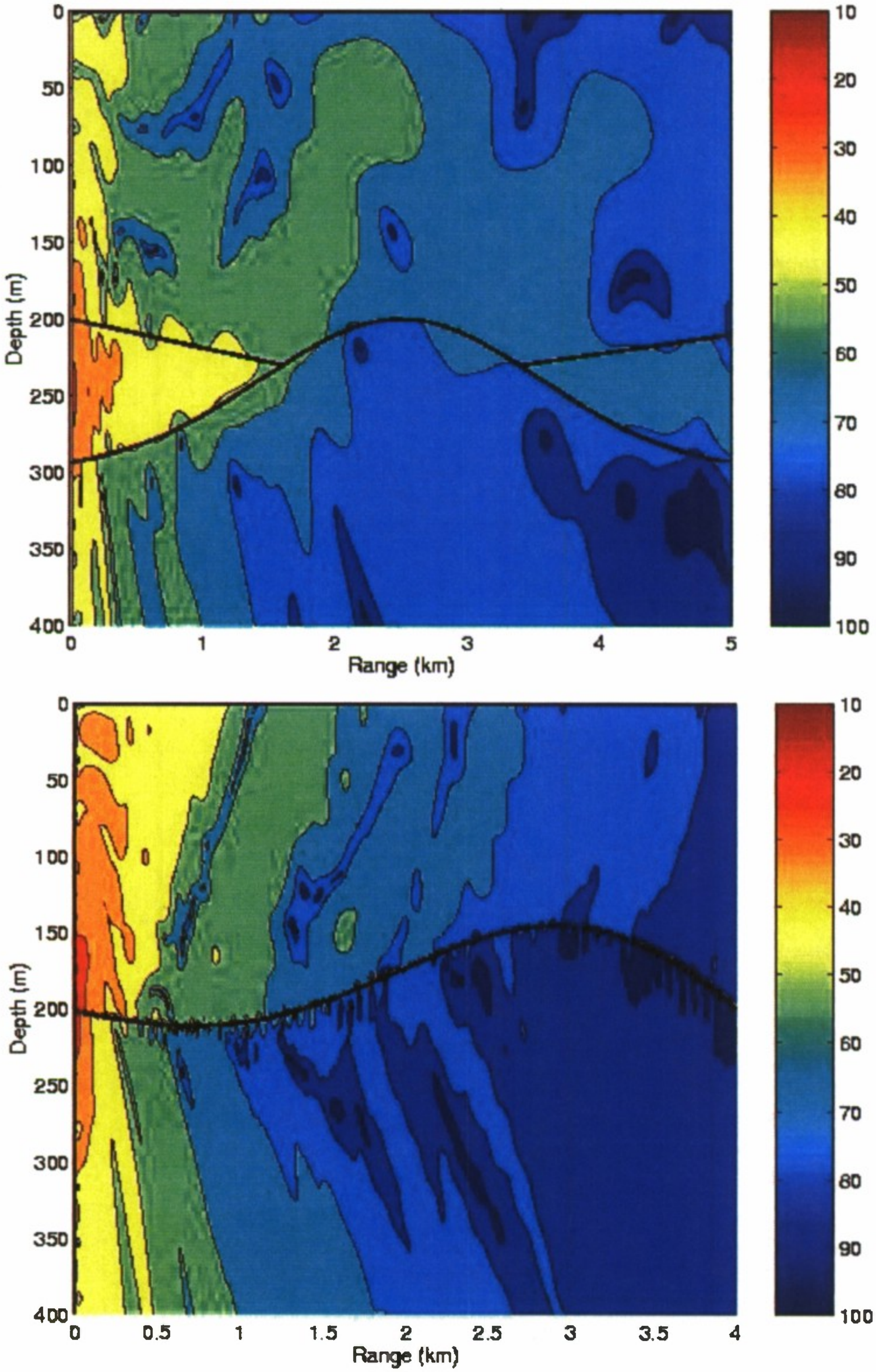
Depth (m)
Range (km)
Depth (m)
Range (km)

Figure 3 (previous page). *Range dependence of layered elastic sediments produces propagation effects that are treated accurately and efficiently by our parabolic equation formulation. Transmission loss contours (to 400 m depth and up to 5 km range) for source frequency 25 Hz are shown for two layered sediments. **Upper:** Three-layer elastic sediment has a middle layer with the lowest sound speeds and a source at 250 m. A dome-type protrusion of the lower interface eliminates the middle layer for about 2 km along the propagation range. The dome forces most of the acoustic energy into the upper layer. Beyond the dome some energy re-enters the middle layer and propagates within this waveguide. **Lower:** Two-layer sediment has the same shear speeds and a strong density contrast, which allows the existence of a Stoneley wave. The interface undulates with a quasi-wavelength of about 4 km. A source at 205 m excites the Stoneley wave, which follows the interface variations as it propagates and decays with depth into both layers.*

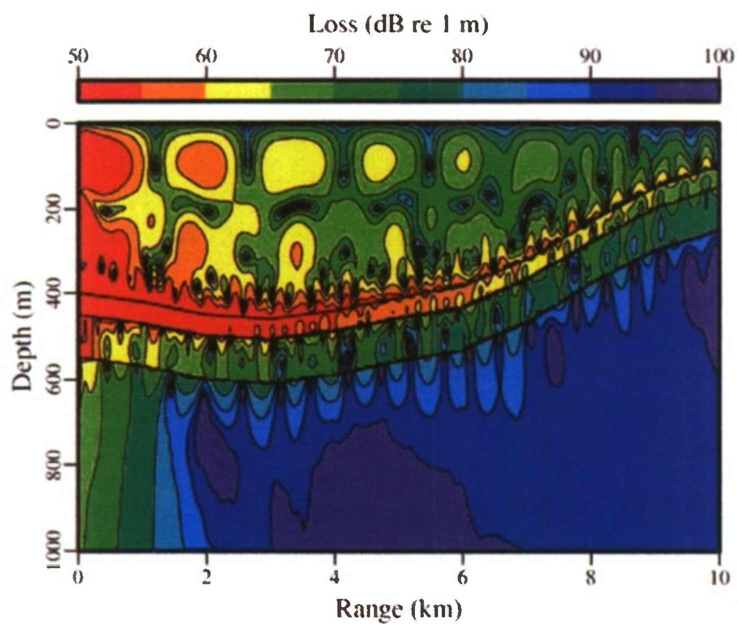

Figure 4. *Propagation over elastic sediments with bathymetry that changes relatively rapidly in wavelength is treated efficiently and accurately by a parabolic equation coordinate-rotation approach. Loss contours on a 50-100 dB scale, to 1000 m in depth and 10 km in range for a 5 Hz source, are shown for a range-dependent layered coastal environment. The ocean depth is 400 m at the source (5 m above the bottom), increases to 460 m at 3 km, and decreases to 100 m at 10 km, changing at least once every 1 km. Two elastic sediment layers, the upper 50 m thick and the lower 100 m, follow the bathymetry and overlay an elastic basement. The upper and lower layers and basement have compressional sound speeds of 1700, 2400, and 3400 m/s, shear speeds of 800, 1200, and 1700 m/s, and density of 1.2, 1.5, and 1.8 g/cm^3. Compressional and shear attenuations in both layers are 0.05 and 0.1 dB/λ and are doubled in the basement. The contours show waveguide propagation in the ocean and in both elastic layers, energy persistence in the basement throughout the upslope region, and a Scholte wave evolving along the water-sediment bathymetry.*

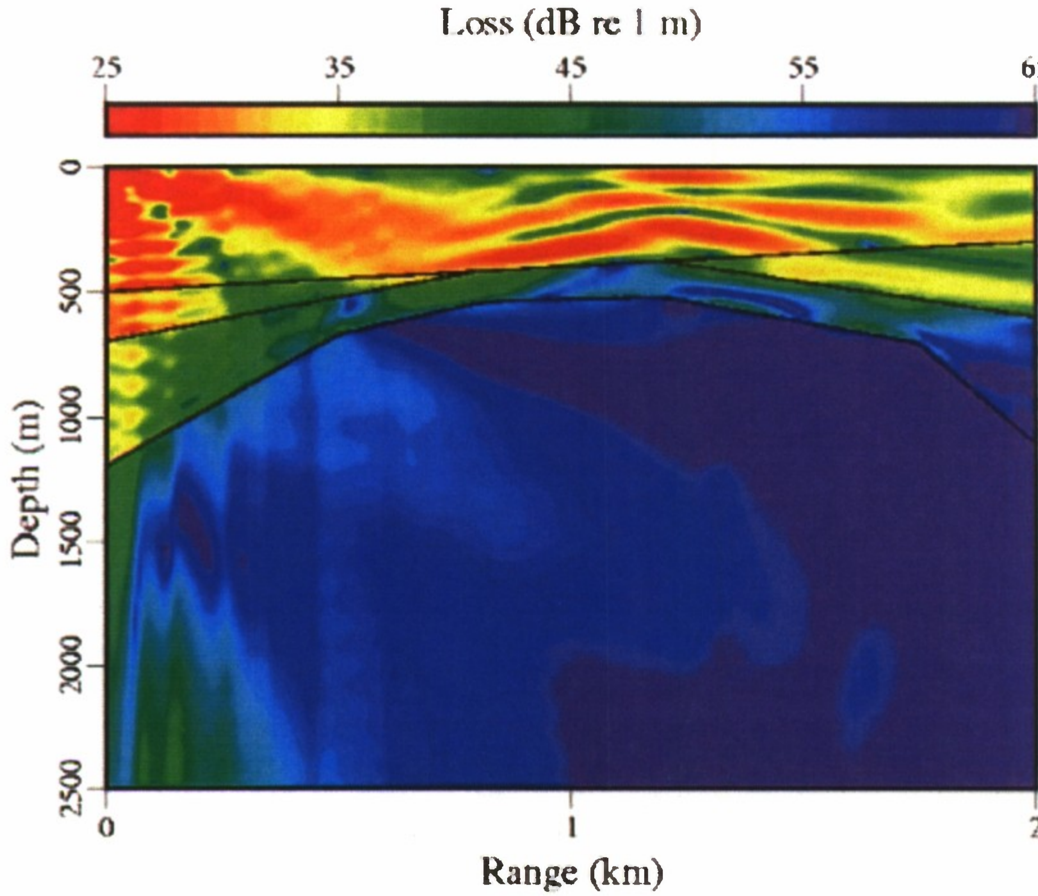

Figure 5. Seismo-acoustic propagation in layered elastic sediments, including substantial range dependence in layer interfaces, is treated efficiently and accurately by our parabolic equation approach that uses single scattering at vertical interfaces. Transmission loss contours on a 25-65 dB scale, to 2500 m depth and 2 km range for a 10 Hz source at 100 m, are shown for a range-dependent layered environment. The first elastic layer decreases from 500 to 400 m over 2 km; the second, with maximum thickness of 300 m, appears as two wedge-shaped regions because it vanishes between 800 and 1200 m in range; the third has depth between 200 and 500 m and boundaries with up to five locations of slope changes; and the fourth is a thick basement. The four layers have compressional sound speeds of 1500, 1700, 2400, and 3400 m/s, shear speeds of 700, 800, 1200, and 1700 m/s, and densities of 1.0, 1.2, 1.5, and 2.5 g/cm^3. Compressional and shear attenuations in the upper layers are 0.1 and 0.2 dB/λ and are doubled in the basement. The calculation requires the extended procedure of our approach, because earlier methods will not converge. The contours show waveguide propagation in the top layer, coupling into and out of the second layer, ducted propagation in the third layer, and weak penetration into the basement.

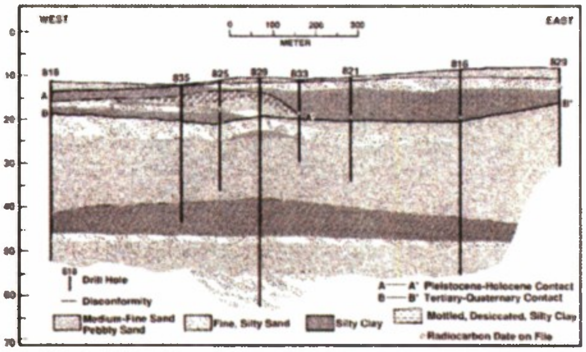

WEST
EAST
0
100
200
300
METER
835
825
833
821
816
A
B
B'
0
10
20
30
40
50
60
70
Drill Hole
Disconformity
A — A' Pleistocene-Holocene Contact
B — B' Tertiary-Quaternary Contact
Medium-Fine Sand
Pebbly Sand
Fine, Silty Sand
Silty Clay
Mottled, Desiccated, Silty Clay
Radiocarbon Date on File

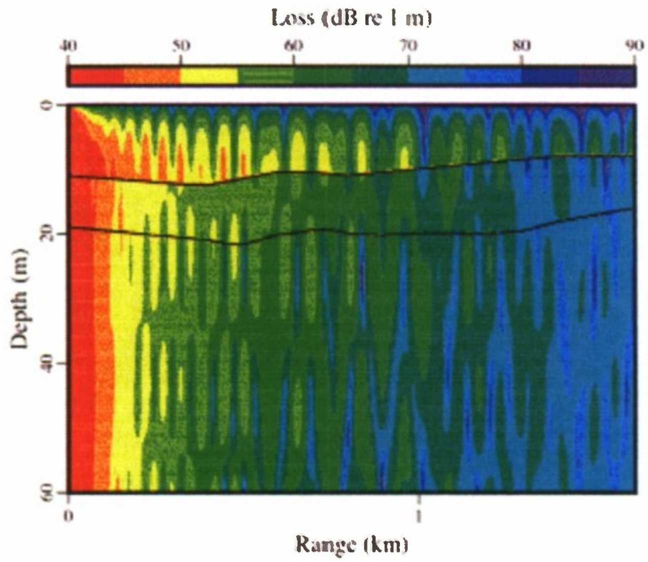

Loss (dB re 1 m)
40
50
60
70
80
90
0
20
40
60
Depth (m)
0
1
Range (km)

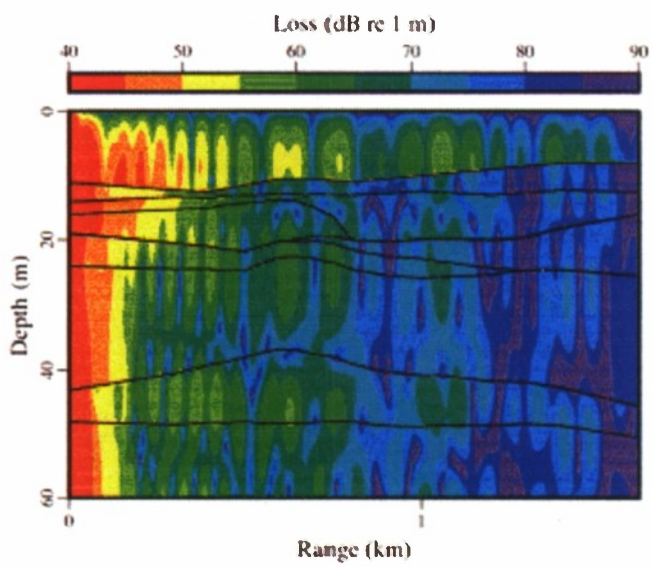

Loss (dB re 1 m)
40
50
60
70
80
90
0
20
40
60
Depth (m)
0
1
Range (km)

Figure 6 (previous page). ***Propagation in waveguides over range dependent elastic sediment layers is handled accurately and efficiently by our parabolic equation approach using coordinate rotations and single scattering corrections. Upper panel: Schematic shows multiple structurally distinct and range dependent layers in 50 m of sediment, below about 10 m of water at the New Jersey AGS site (courtesy Dr. M. Badiey). Vertical lines indicate borehole locations. Middle panel: Color contours are transmission loss between 40 and 90 dB (re: 1 m) over 60 m depth and 1.6 km range for a 50 Hz source at 5 m. The sediment model has two homogeneous elastic layers with range dependent interface and bathymetry. Considerable energy propagates in the water and the top sediment layer. Lower panel: Corresponding contours when the bottom model has eight homogeneous elastic layers with range dependence based closely on the schematic. Considerably less energy propagates in the water and the sediment layer in this case. Realistic range dependent elastic sediment layer structure can significantly affect propagation in shallow water waveguides.***

Figure 7 (next page). ***Shallow water propagation over range dependent elastic sediment layers and into a beach is handled accurately and efficiently by a parabolic equation solution using coordinate rotations and single scattering corrections. Upper panel: Color contours are transmission loss between 40 and 90 dB (re: 1 m) over 200 m depth and 2.5 km range for a 150 Hz source at 30 m. The ocean at the source has depth 60 m and decreases with variable slope to zero at 1.8 km, followed by a beach rising to 18 m at 2.5 km; the two elastic sediment layers have constant thicknesses of 11 and 63 m and track the bathymetry to 1.8 km; the bottom layer is an elastic basement. Energy propagates from the ocean into both sediment layers and up the beach. Middle panel: Corresponding loss curves at 30 m depth. The dashed curve is a benchmark full field finite-element solution, and the solid curve is calculated from our variable rotated method. The two curves agree very well, with differences within 1 dB. Lower panel: Corresponding loss curves with the solid curve calculated from a coordinate mapping method, which is the only other one capable of handling propagation into and up a beach over elastic sediments. The two curves differ in pattern phase and level by several dB in the topography region. Our method is accurate and effective for propagation with range dependent elastic sediments and topography.***

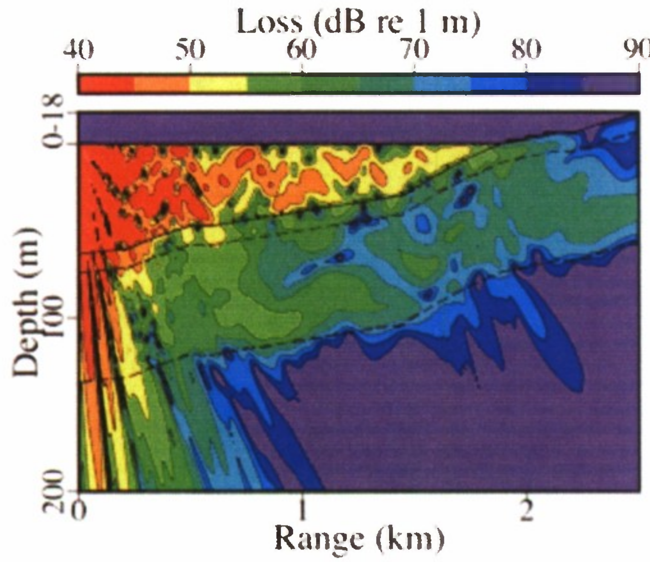

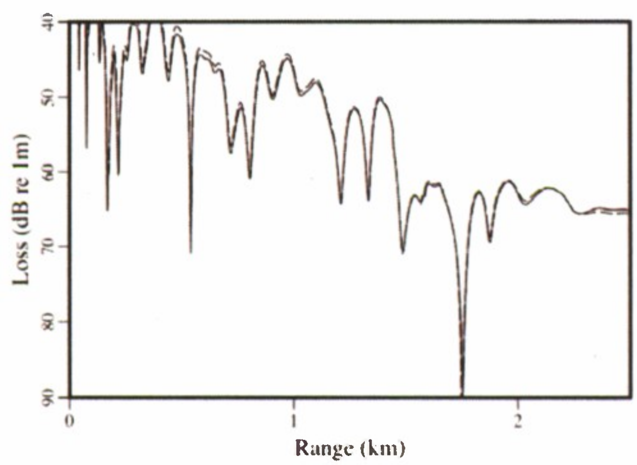

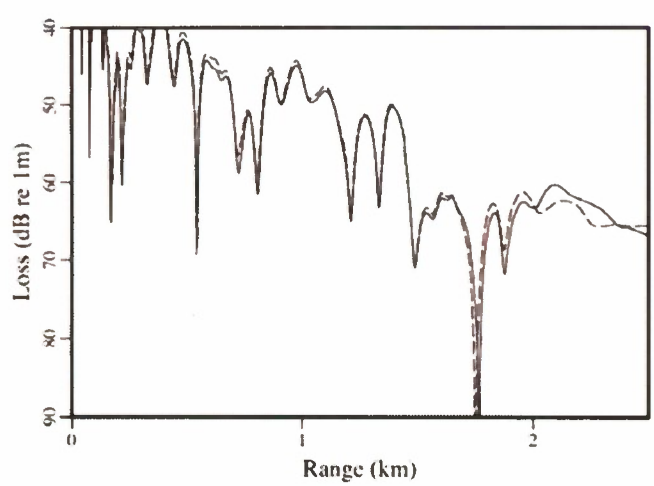

B. Environmental Features, Acoustic Effects, and Data Comparisons

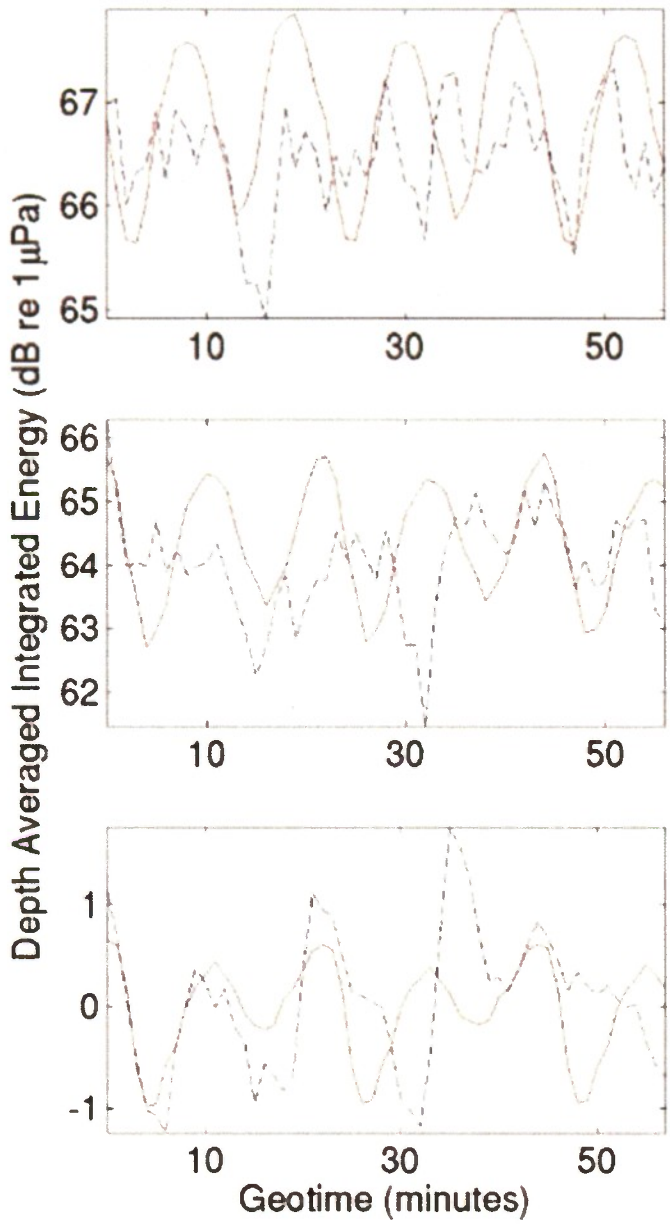

<u>Figure 8.</u> The quantitative influence of internal solitons on time variability of received broadband signals can be found from parabolic equation computations. In the SWARM95 experiment, signals from an air gun source on the R/V Cape Hatteras were received at the NRL VLA. Curves show depth-averaged signal-integrated energy from observations [blue dashed] and computations [red solid] over about sixty minutes. <u>Upper</u>: Energy in a 10-Hz band centered at 32 Hz. The simulations show oscillations of about 12 min period and 2 dB amplitude. The data has similar and somewhat noisier behavior. <u>Middle</u>: Same, except with frequency band centered at 64 Hz [overall band energy is lower by about 2.5 dB]. The oscillation amplitudes extend up to about 3 dB. <u>Lower</u>: Same, except with bands 10-250 Hz [data] and 10-150 Hz [computations], with curves plotted about mean energy [total amplitude variation 2 to 3 dB]. The variability arises from coupling between wav enumbers from soliton energy spectrum peaks and dominant acoustic modes.

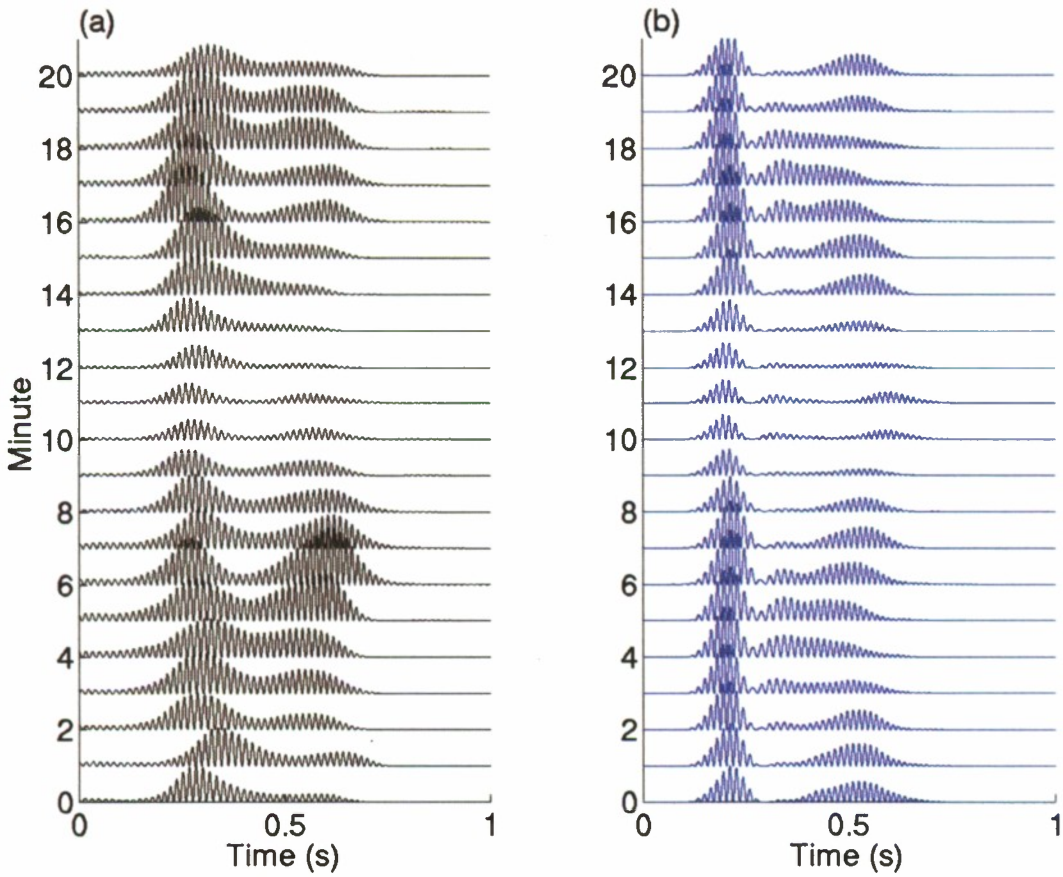

<u>Figure 9</u>. Horizontal refraction of acoustic energy can be identified, using parabolic equation computations, as the mechanism that produces time variability of observed broadband signals. During the SWARM95 experiment, signals from an air gun source on R/V Cape Hatteras were received at the WHOI VLA. Each black or blue curve shows the amplitude of the signal at hydrophone 2, at depth 19 m, over a one-second window. Each curve is the filtered output from a 10-Hz band centered at 32 Hz. Each column of curves corresponds to shots every minute during a twenty-minute window. <u>Left panel</u>: Black curves are observational data showing two mode arrivals. Amplitudes of both modes increase to relatively large values during the first seven minutes, then over the next seven minutes decrease to much smaller values (by about a factor of three for mode 1, ten for mode 2), and finally return to large values over the last six minutes. The second-mode-arrival delay times are initially short, then increase, and finally decrease. The variations in signal amplitude correspond to those seen in the pulse-integrated energy, which are about 6 dB. <u>Right panel</u>: Blue curves are from PE simulations when internal soliton wave fronts form an angle of 3 degrees with the propagation track. The variability in simulation amplitudes and delay times show the same features (with less noise) as the data.

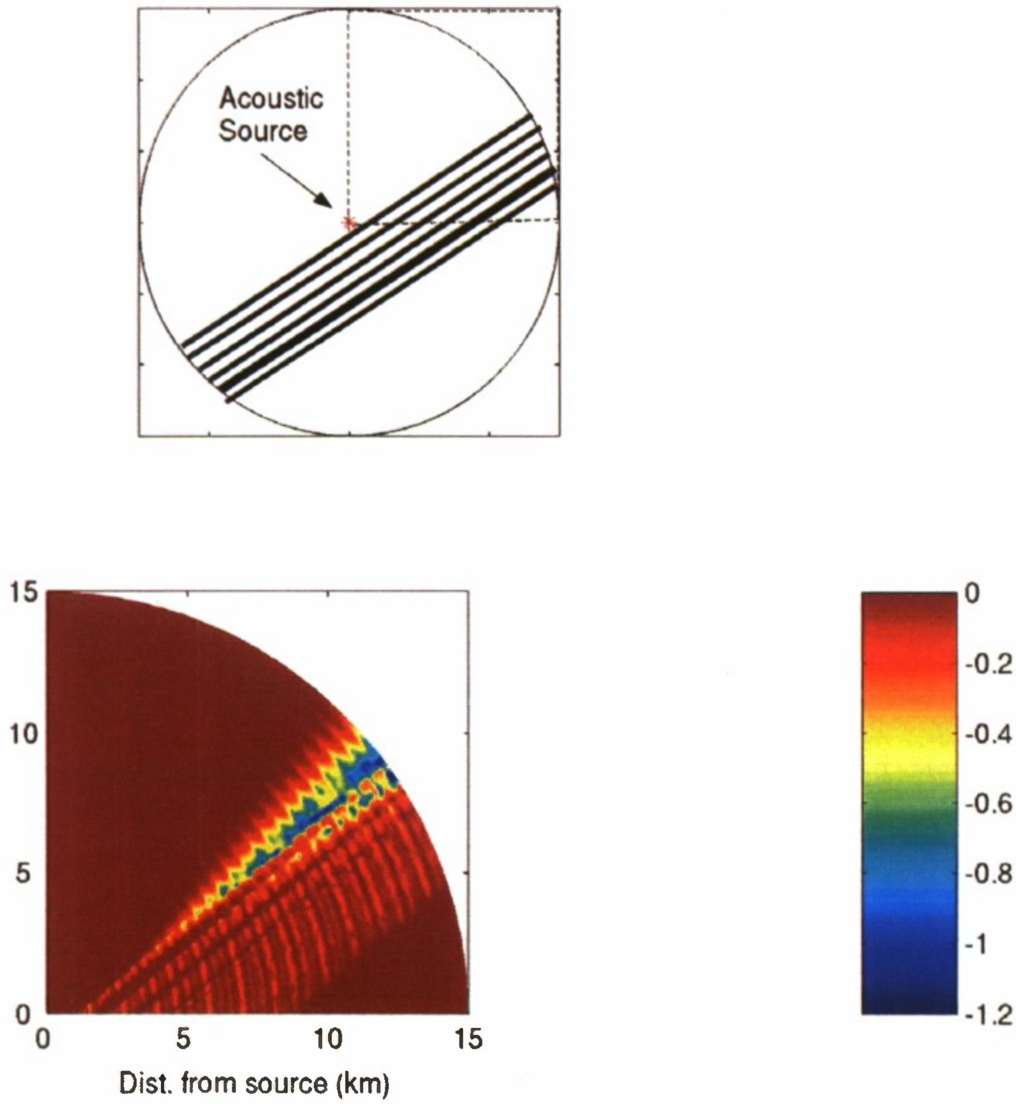

Figure 10*. Random variations in internal soliton properties produce significant intensity variability for low-angle propagation near soliton wave fronts. *Upper panel*: Schematic of a horizontal circular domain of radius 15 km with an acoustic source at the center. A packet of six $sech^2$ soliton pulses, each with mean amplitude 12 m and width 270 m, has its leading edge 100 m from the source and 620 m separations between pulses. Each pulse has a random amplitude variation with standard deviation 3 m, along with a corresponding width variation. *Lower panel*: Contours in the boxed quadrant of the domain for intensity scintillation index (SI) on a 0-1.2 scale, at frequency 55 Hz. The SI is calculated by averaging 50 realizations from an adiabatic mode PE, using water depth 100 m and range-independent profiles of water sound speed and geoacoustic parameters typical of southwest SWARM tracks. Substantial SI variability occurs primarily in two locations: ahead of the leading pulse, which is the location of an interference pattern analogous to Lloyd's Mirror, and in the duct formed by the leading and subsequent pulses. As range increases the maximum SI value tends to increase and to spread azimuthally in front of the leading soliton.

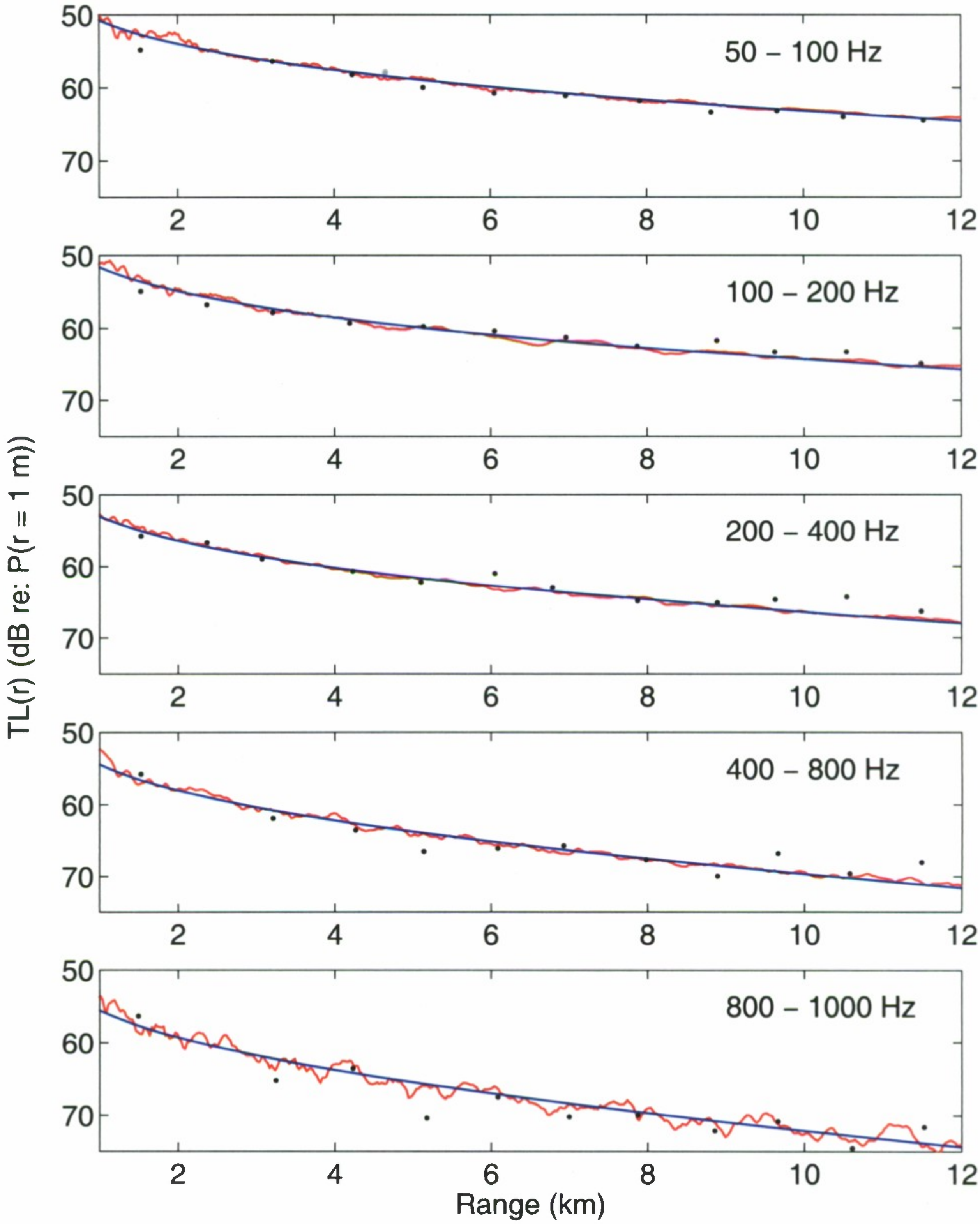

50 – 100 Hz
100 – 200 Hz
200 – 400 Hz
400 – 800 Hz
800 – 1000 Hz
TL(r) (dB re: P(r = 1 m))
Range (km)
50
60
70
2
4
6
8
10
12

<u>Figure 11 (previous page)</u>. Shallow water propagation can be modeled across frequency bands when fairly limited critical oceanic and geoacoustic information is available. Each of the five plots shows transmission loss versus range (to 12 km) for Leg 3 at Site 1 of ACT III in the Strait of Korea, averaged over a frequency band (50-100, 100-200, 200-400, 400-800, and 800-1000 Hz). Dots (roughly every km) represent experimental data. Parabolic equation simulations (red curves) are obtained using available sound speed profiles and bathymetry data and a geoacoustic model developed previously for another experimental leg. The upper sediment layer attenuation depends on frequency to the 1.8 power. Fits to the simulations based on cylindrical spreading plus linear effective attenuation (blue curves) are included. For all five frequency bands, the agreement shown between experimental data and calculated results is excellent. Similar agreement is obtained between independent narrowband data for five frequencies and corresponding simulations, provided the nonlinear sediment attenuation is retained.

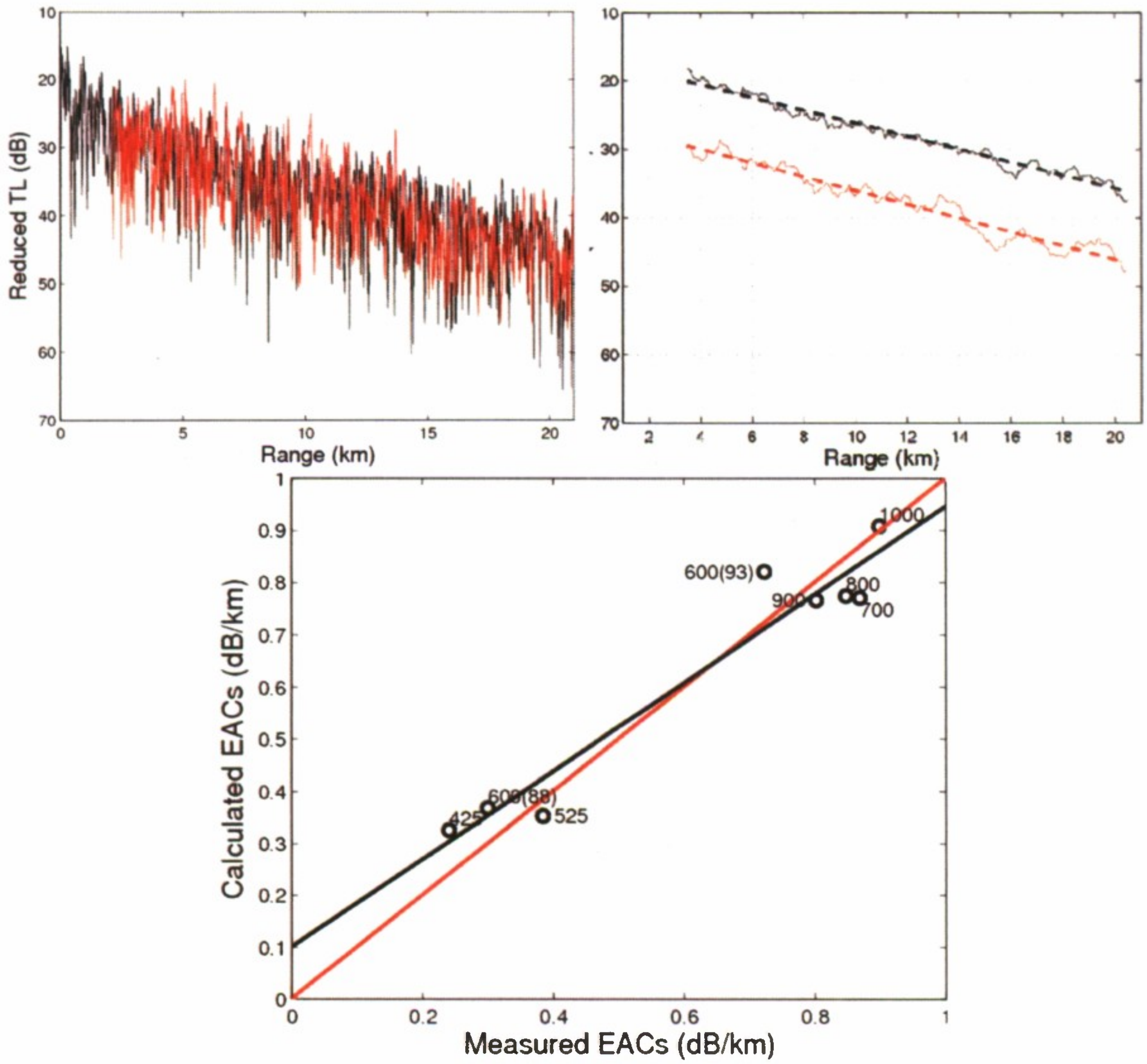

<u>Figure 12</u>. Transmission loss degradation in regions with moderate range dependence and sandy-silty sediments is modeled effectively by accounting for water profiles, bathymetry, and key features of the upper sediment attenuation. <u>Upper panels: (left)</u> Transmission loss curves with cylindrical spreading removed; PE calculations (red) and measurements from 1993 ACT II experiment (black), to range 21 km and at depth 53 m. Highly oscillatory interference patterns occur from many propagating modes. <u>(right)</u> Range-averaged (1 km window) and depth-averaged (three receivers) reduced loss curves and best linear fits, with calculations displaced 10 dB. The slopes are the effective attenuation coefficients (EACs); 1.01 (measured) and 0.95 (calculated). <u>Lower panel</u>: Scatter plot of measured and calculated EACs (with frequencies labeled) from ACT II and the 1988 New Jersey Shelf experiment. Calculations use sediment attenuation frequency-power exponent 1.8 and surface value 0.35. The best linear fit to the points is the line (black) with slope 0.85 and intercept 0.10, which is close to the exact-model line (red).

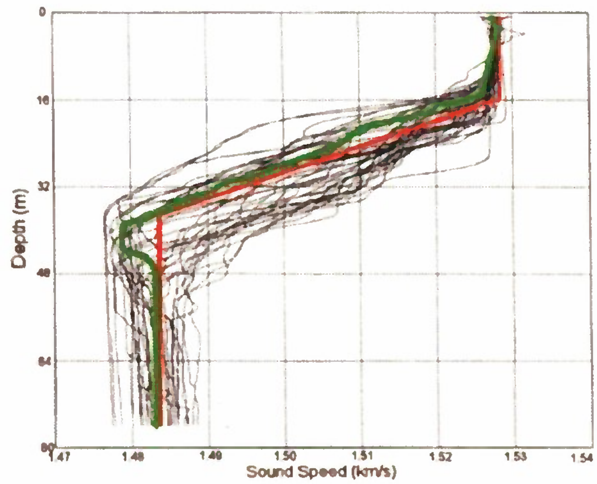
Depth (m)
Sound Speed (km/s)

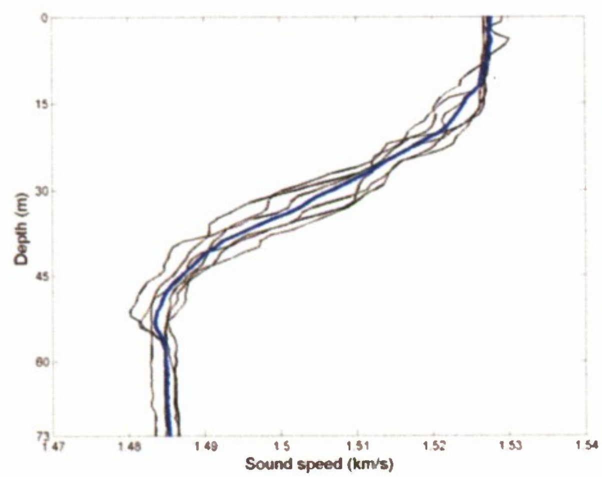
Depth (m)
Sound speed (km/s)

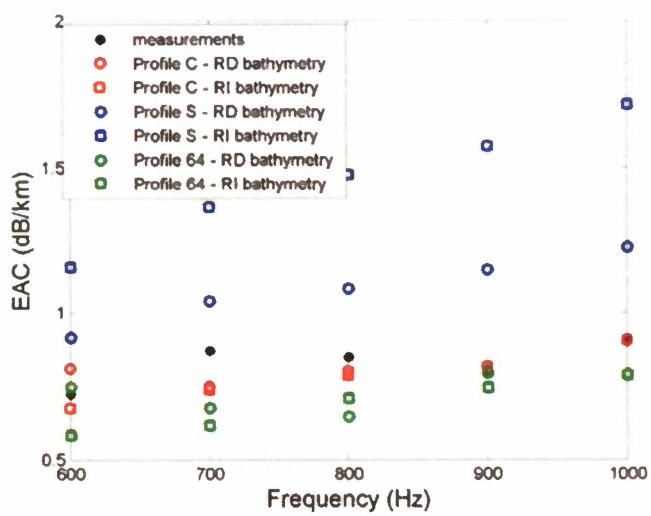
measurements
Profile C - RD bathymetry
Profile C - RI bathymetry
Profile S - RD bathymetry
Profile S - RI bathymetry
Profile 64 - RD bathymetry
Profile 64 - RI bathymetry
EAC (dB/km)
Frequency (Hz)

Figure 13 (previous page)*. An effective attenuation coefficient (EAC) metric for overall transmission-loss decrease is tested for sensitivity to water sound speed profiles and bathymetry, in regions of sandy-silty sediments and moderate range dependence. *Upper panel*: Measured profiles (black) over 73 m depth and 1475 to 1530 m/sec from the 1993 ACT II experimental site, a composite profile C (red) that represents the principal thermocline feature from 16 to 36 m, and the profile 64 (green) that is nearest the source location. *Middle panel*: Sample of six measured profiles (black) for one experimental run and their depth average profile S (blue). Among all measured profiles, the sample profiles have deep thermoclines. *Lower panel*: EACs in dB/km for five experimental frequencies from 600 to 1000 Hz. EACs from measurements (black) compare well with calculations using profiles C (red) or 64 (green) and either range dependent or range independent average bathymetry. EACs from measurements generally do not compare well with calculations (blue) using profile S or (not shown) the range dependent sample. At low frequencies the EAC metric is sensitive to the average water profile and insensitive to moderate range dependence in water profiles and bathymetry.

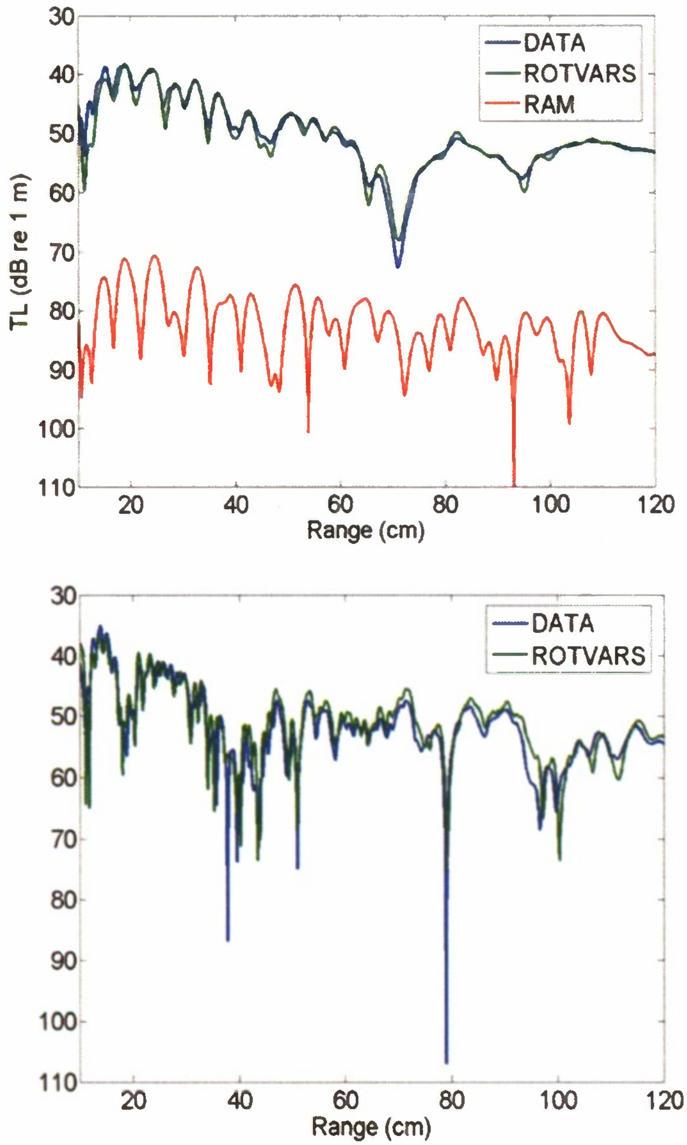

<u>Figure 14</u>. Propagation in range-dependent oceanic waveguides over elastic sediments is treated efficiently and accurately by our parabolic equation approach that uses coordinate rotations at ranges where the bathymetry slope changes. High-quality data obtained from a tank experiment at NRL provides transmission loss curves, shown for source and receiver depths 1.5 and 6.3 cm, for propagation over an elastic slab sloped from 13.3 to 4.5 cm depth on a 120 cm range. The slab has nominal compressional and shear sound speeds of 2290 and 1050 m/s, attenuations of 0.76 and 1.05 dB/λ, and density 1.378 g/cm^3. The blue curves are processed data and the green curves are calculations. <u>Upper panel</u>: For 100 kHz, the amplitudes and phases of the loss patterns for data and calculations show excellent agreement. The red curve displayed (and displaced 30 dB) is for a fluid-model bottom, which differs strongly in all respects from the data. <u>Lower panel</u>: For 300 kHz with many more modes, fine details of the interference patterns for data and calculations agree.

IV. PHD STUDENTS GRADUATED

[0] **S. D. Frank**, "Analysis and Modeling of Ocean Acoustic Effects from Nonlinear Internal Waves," September 2003 (co-advisor M. Badiey) (start of grant period).
Initial position: Assistant Professor, Marist College, Poughkeepsie, NY
Current position: Associate Professor, Marist College, Poughkeepsie, NY

[1] **D. A. Outing,** "Parabolic Equation Techniques for Range-Dependent Elastic Media," May 2004 (co-advisor M. D. Collins).
Initial position: Assistant Professor, United States Military Academy, West Point, NY
Current position: Associate Professor and Academy Professor, USMA, West Point, NY

[2] **E. T. Kusel**, "New Parabolic Equation Solutions for High Frequency and Elastic Media Problems," May 2005 (co-advisor M. D. Collins).
Initial position: Postdoctoral Assistant, Graduate School of Oceanography, University of Rhode Island, Narragansett, RI
Current position: Research Assistant, Hatfield Marine Science Center, Oregon State University, Newport, OR

[3] **J. M. Collis**, "New Parabolic Equation Solutions for Elastic Media," August 2006 (co-advisor M. D. Collins).
Initial position: ONR Postdoctoral Fellow in Ocean Acoustics, Woods Hole Oceanographic Institution, Woods Hole, and Boston University, Boston, MA
Current position: Assistant Professor, Colorado School of Mines, Golden, CO

[4] **L. K. Reilly-Raska**, "Deterministic and Stochastic Internal Wave Effects on Shallow Water Acoustic Propagation," January 2007 (co-advisor J. F. Lynch).
Initial position: Postdoctoral Associate, Rensselaer Polytechnic Institute, Troy, NY
Current position: Scientific Staff, Lincoln Laboratory, Lexington, MA

[5] **S. M. Dediu**, "Analysis of Frequency Dependent Attenuation in Shallow Water," August 2007 (co-advisor W. M. Carey).
Initial position: Postdoctoral Assistant, North Carolina State University, Raleigh, NC

[6] **W. Saintval,** "Influence of Modal Attenuation on Shallow Water Propagation," August 2008 (co-advisor W. M. Carey).
Initial position: Postdoctoral Assistant, Rosenstiel School of Marine and Atmospheric Sciences, University of Miami, Miami, FL
Current position: Scientific Staff, Naval Research Laboratory, Washington, DC

V. PUBLICATIONS

[1] W. Jerzak, W. L. Siegmann, and M. D. Collins, "Modeling Rayleigh and Stoneley waves and other interface and boundary effects with the parabolic equation," *J. Acoust. Soc. Am.* **117**, 3497-3503 (2005).

[2] D. A. Outing, W. L. Siegmann, and M. D. Collins, "Scholte-to-Rayleigh conversion and other range-dependent effects in elastic media," *IEEE J. Ocean Eng.* **32**, 620-625 (2007).

[3] D. A. Outing, W. L. Siegmann, M. D. Collins and E. K. Westwood, "Generalization of the rotated parabolic equation to variable slopes," *J. Acoust. Soc. Am.* **120**, 3534-3538 (2006).

[4] E. T. Kusel, W. L. Siegmann, and M. D. Collins, "A single-scattering correction for large contrasts in elastic layers," *J. Acoust. Soc. Am.* **121**, 808-813 (2007).

[5] J. M. Collis, W. L. Siegmann, F. B. Jensen, M. Zampolli, E. T. Kusel, and M. D. Collins, "Parabolic equation solution of seismo-acoustic problems involving variations in bathymetry and sediment thickness," *J. Acoust. Soc. Am.* **123,** 51-58 (2008).

[6] E. T. Kusel, W. L. Siegmann, and M. D. Collins, "The split-step Pade-Fourier solution," *Acta Acustica united with Acustica*, **93**, 43-48 (2008).

[7] J. M. Collis, W. L. Siegmann, M. Zampolli, and M. D. Collins, "Extension of the rotated elastic parabolic equation to beach and island propagation," *IEEE J. Ocean. Eng.*, **34**, 617-623 (2009).

[8] M. D. Collins, H. J. Simpson, R. J. Soukup, J. M. Collis, E. T. Kusel, W. Jerzak, D. A. Outing, and W. L. Siegmann, "Parabolic equation techniques for range-dependent seismo-acoustics," *Second Conf. Math. Modeling Wave Phenom.*, Sweden, *AIP Conf. Proc.* **834**, 130-138 (2006).

[9] M. D. Collins, F. B. Jensen, P. L. Nielsen, M. Zampolli, H. Schmidt, and W. L. Siegmann, "Range-dependent seismo-acoustic benchmark problems," *Proc. Eighth Euro. Conf. Underwater Acoust.*, Portugal, 56-63 (2006).

[10] F. B. Jensen, P. L. Nielsen, M. Zampolli, M. D. Collins, and W. L. Siegmann, "Benchmark scenarios for range-dependent seismo-acoustic models," *Proc. Eighth Int. Conf. Theoret. Comp. Acoust.*, Crete, I-5, 8 pp. (2007).

[11] S. D. Frank, M. Badiey, J. F. Lynch, and W. L. Siegmann, "Analysis and modeling of broadband air gun data influenced by nonlinear internal waves," *J. Acoust. Soc. Am.* **116**, 3404-3422 (2004).

[12] S. D. Frank, M. Badiey, J. F. Lynch, and W. L. Siegmann, "Experimental evidence of threc-dimensional acoustic propagation caused by nonlinear internal waves." *J. Acoust. Soc. Am.* **118**, 723-734 (2005).

[13] M. Badiey, B. Katsnelson, J. F. Lynch, S. Pereselkov, and W. L. Siegmann, "Thrce-dimensional intensity variability in shallow water in the presence of internal waves in the SWARM 95 experiment," *J. Acoust. Soc. Am.* **117**, 613-625 (2005).

[14] J. F. Lynch, J. A. Colosi, G. G. Gawarkiewicz, T. F. Duda, A. D. Pierce, M. Badiey, B. Katsnelson, J. E. Miller, W. L. Siegmann, C.-S. Chiu, and A. Newhall, "Consideration of fine-scale coastal oceanography and 3-D acoustic effects for the ESME sound exposure model," *IEEE J. Ocean Eng.* **31**, 33-48 (2006).

[15] W. M. Carey, J. F. Lynch, W. L. Siegmann, I. Rozenfeld, and B. J. Sperry, "Sound transmission and spatial coherence in selected shallow water areas: measurement and theory," *J. Comp. Acoust.* **14**, 265-298 (2006).

[16] J. D. Holmes, W. M. Carey, S. M. Dediu, and W. L. Siegmann, "Nonlinear frequency-dependent attenuation in sandy sediments," *J. Acoust. Soc. Am.* **121**, EL218-EL222 (2007).

[17] S. M. Dediu, W. L. Siegmann, and W. M. Carey, "Statistical analysis of sound transmission results obtained on the New Jersey continental shelf," *J. Acoust. Soc. Am.*, **122**, EL23-EL28 (2007).

[18] J. M. Collis, W. L. Siegmann, M. D. Collins, H. J. Simpson, and R. J. Soukup. "Comparison of propagation calculations and data from a scismo-acoustic tank experiment," *J. Acoust. Soc. Am.* **122**, 1987-1993 (2007).

[19] A. D. Pierce, W. M. Carey, W. L. Siegmann, S. V. Kaczkowski, and W. Saintval, "Analytic solution for guided waves in a canonical model of shallow water with a theromcline," *Proc. IEEE Oceans 06 Conf.*, Boston, DOI306891, 7 pp. (2006).

[20] W. Saintval, W. L. Siegmann, W. M. Carey, J. D. Holmes, and A. D. Pierce, "Sensitivity of modal attenuation coefficients to environmental variability," *Proc. IEEE Oceans 06 Conf.*, Boston, DOI306872, 3 pp. (2006).

[21] S. V. Kaczkowski, A. D. Pierce, W. M. Carey, and W. L. Siegmann, "Modal approximations in shallow water," *Proc. IEEE Oceans 07 Conf.*, Aberdeen, DOI4302472, 6 pp. (2007).

[22] M. D. Collins and W. L. Siegmann, *Parabolic Wave Equations with Applications*, draft prcpared for Springer-Verlag.

VI. PRESENTATIONS

[1] D. A. Outing, W. L. Siegmann, and M. D. Collins, "Generalization of the rotated parabolic equation to variable slopes," *146th Meet. Acoust. Soc. Am.,* Cancun, (A) *J. Acoust. Soc. Am.* **114**, 2428 (2003).

[2] E. T. Kusel, W. L. Siegmann, and M. D. Collins, "Energy-conserving and single-scattering parabolic equation solutions for elastic media," *146th Meet. Acoust. Soc. Am.,* Cancun, (A) *J. Acoust. Soc. Am.* **114**, 2428 (2003).

[3] L. K. Reilly-Raska, J. A. Colosi, J. F. Lynch, T. F. Duda and W. L. Siegmann, "Intensity fluctuations from deterministic and random azimuthal variability," *146th Meet. Acoust. Soc. Am.,* Cancun, (A) *J. Acoust. Soc. Am.* **114**, 2461 (2003).

[4] W. M. Carey, J. F. Lynch, W. L. Siegmann, I. Rozenfeld, and B. J. Sperry, "Sound transmission and spatial coherence in selected shallow water areas: measurement and theory," (A) *Sixth Int. Conf. Theoret. and Comp. Acoust.*, Honolulu (October 2003).

[5] D. A. Outing, W. L. Siegmann, and M. D. Collins, "A variable rotated parabolic equation for elastic media," *147th Meet. Acoust. Soc. Am.,* New York City (A) *J. Acoust. Soc. Am.* **115**, 2579 (2004).

[6] L. K. Reilly-Raska, J. F. Lynch, J. A. Colosi, T. F. Duda, and W. L. Siegmann, "Acoustic effects from the horizontal variability spectrum of nonlinear internal waves," New York City, *147th Meet. Acoust. Soc. Am.,* (A) *J. Acoust. Soc. Am.* **115**, 2549 (2004).

[7] W. L. Siegmann, "New parabolic equations for elastic media," *Naval Research Laboratory,* Washington DC (June 2004).

[8] W. L. Siegmann, "Parabolic equations for propagation applications in sediments," *Office of Naval Intelligence,* Suitland (September 2004).

[9] E. T. Kusel, W. L. Siegmann, and M. D. Collins, "A single-scattering solution that handles large contrasts across interfaces," *148th Meet. Acoust. Soc. Am.,* San Diego (A) *J. Acoust. Soc. Am.* **116**, 2549 (2004).

[10] L. K. Reilly-Raska, W. L. Siegmann, J. F. Lynch, J. Colosi, and T. F. Duda, "Acoustic mode coupling effects from propagation through nonlinear internal waves," *148th Meet. Acoust. Soc. Am.,* San Diego (A) *J. Acoust. Soc. Am.* **116**, 2535 (2004).

[11] J. Bruch, M. D. Collins, D. K. Dacol, J. F. Lingevitch, and W. L. Siegmann, "A parabolic equation for advected acousto-gravity waves," *148th Meet. Acoust. Soc. Am.,* San Diego (A) *J. Acoust. Soc. Am.* **116**, 2516 (2004).

[12] J. M. Collis, W. L. Siegmann, M. D. Collins, H. J. Simpson, and R. J. Soukup. "Tank experiments and model comparisons of shallow water acoustic propagation over elastic

bottoms," *149th Meet. Acoust. Soc. Am.*, Vancouver, (A) *J. Acoust. Soc. Am.* **117**, 2576 (2005).

[13] S. D. Frank, J. F. Lynch, M. Badiey, and W. L. Siegmann, "Influence of random nonlinear internal wave parameters on resonant acoustic mode coupling," *149th Meet. Acoust. Soc. Am.,* Vancouver, (A) *J. Acoust. Soc. Am.* **117**, 2547 (2005).

[14] W. Saintval, W. L. Siegmann, W. M. Carey, A. D. Pierce, and J. F. Lynch, "Dependence of modal attenuation coefficient frequency variation on upper sediment attenuation," *149th Meet. Acoust. Soc. Am.,* (A) *J. Acoust. Soc. Am.* **117**, 2496 (2005).

[15] W. Saintval, W. L. Siegmann, W. M. Carey, A. D. Pierce, and J. F. Lynch, "Frequency dependence of modal attenuation coefficients from a simplified Biot sediment model," *Walter L. Hawkins Res. Conf., RPI,* Troy (2005).

[16] W. L. Siegmann, R. Krysko, M. D. Collins, and L. T. Fialkowski, "Vector intensity calculations using the parabolic wave equation," *ONR Workshop on Vector Sensors,* Arlington (September 2005).

[17] J. M. Collis, W. L. Siegmann, and M. D. Collins, "Extension of the variable rotated parabolic equation to problems involving variable topography," *150th Meet. Acoust. Soc. Am.,* Minneapolis, (A) *J. Acoust. Soc. Am.* **118**, 1970 (2005).

[18] M. D. Collins, F. B. Jensen, P. L. Nielsen, M. Zampolli, H. Schmidt, and W. L. Siegmann, "Range-dependent seismo-acoustics benchmark problems," *150th Meet. Acoust. Soc. Am.,* Minneapolis, (A) *J. Acoust. Soc. Am.* **118**, 1970 (2005).

[19] W. L. Siegmann, "Recent progress in parabolic equations for acoustic propagation," *U. S. Military Academy,* West Point (March 2006).

[20] J. M. Collis, W. L. Siegmann, and M. D. Collins, "Propagation in highly range-dependent shallow-water waveguides with elastic sediments and beach interactions," *151st Meet. Acoust. Soc. Am.,* Providence, (A) *J. Acoust. Soc. Am.* **119**, 3344 (2006).

[21] W. Saintval, W. L. Siegmann, W. M. Carey, A. D. Pierce, and J. F. Lynch, "Properties of modal attenuation coefficients in shallow water upper sediments," *Soc. Ind. Appl. Math. Meet.*, Boston (July 2006).

[22] S. M. Dediu, W. M. Carey, and W. L. Siegmann, "Propagation predictability on the New Jersey Shelf," *IEEE Oceans 06 Conf.,* Boston (September 2006).

[23] W. Saintval, W. L. Siegmann, W. M. Carey, J. D. Holmes, and A. D. Pierce, "Sensitivity of modal attenuation coefficients to environmental parameters," *IEEE Oceans 06 Conf.*, Boston (September 2006).

[24] A. D. Pierce, W. M. Carey, W. L. Siegmann, S. V. Kaczkowski, and W. Saintval, "Analytical solution for guided waves in a canonical model of shallow water with a thermocline," *IEEE Oceans 06 Conf.*, Boston (September 2006).

[25] P. L. Nielsen, F. B. Jensen, M. Zampolli, M. D. Collins, and W. L. Siegmann, "Benchmarking range-dependent seismo-acoustic propagation problems," *152nd Meet. Acoust. Soc. Am.,* Honolulu, (A) *J. Acoust. Soc. Am.* **120**, 3182 (2006).

[26] J. M. Collis and W. L. Siegmann, "Benchmarking the variable rotated and mapping parabolic equation solutions," *153rd Meet. Acoust. Soc. Am.,* Salt Lake City, (A) *J. Acoust. Soc. Am.* **121**, 3075 (2007)

[27] W. Saintval, W. L. Siegmann, W. M. Carey, and A. D. Pierce, "Frequency variability of modal attenuation coefficients," *153rd Meet. Acoust. Soc. Am.,* Salt Lake City, (A) *J. Acoust. Soc. Am.* **121**, 3076 (2007).

[28] S. M. Dediu, W. M. Carey, A. D. Pierce, and W. L. Siegmann, "Sediment attenuation effects in sound transmission results from the New Jersey continental shelf," *153rd Meet. Acoust. Soc. Am.,* Salt Lake City, (A) *J. Acoust. Soc. Am.* **121**, 3126 (2007).

[29] M. D. Collins, W.-Y. Jung, E. T. Kusel, and W. L. Siegmann, "Efficient modeling of range-dependent seismo-acoustics problems," *154th Meet. Acoust. Soc. Am.,* New Orleans, (A) *J. Acoust. Soc. Am.* **122,** 2942 (2007).

[30] S. V. Kaczkowski, W. L. Siegmann, A. D. Pierce, and W. M. Carey, "Mode formulas for shallow water waveguides using a modified asymptotic approximation," *154th Meet. Acoust. Soc. Am.,* New Orleans, (A) *J. Acoust. Soc. Am.* **122**, 2942 (2007).

[31] W. Saintval, W. M. Carey, A. D. Pierce, J. F. Lynch, and W. L. Siegmann, "Environmental effects on frequency behavior of modal attenuation coefficients for sandy bottoms," *155th Meet. Acoust. Soc. Am.,* Paris, (A) *J. Acoust. Soc. Am.* **123**, 3594 (2008).

[32] J. M. Collins, M. D. Collins, H. J. Simpson, R. J. Soukup, and W. L. Siegmann, "Shallow-water tank experiments and model comparisons over range-dependent elastic bottoms," *155th Meet. Acoust. Soc. Am.,* Paris, (A) *J. Acoust. Soc. Am.* **123**, 3602 (2008).

[33] A. M. Metzler, W. L. Siegmann, M. D. Collins, R. A. Zingarelli, and S. A. Chin-Bing, "Time-domain solutions for Rayleigh and Stoneley waves using the single-scattering parabolic equation," *156th Meet. Acoust. Soc. Am.,* Miami, (A) *J. Acoust. Soc. Am.* **124**, 2585 (2008).

[34] C. C. Boughan, T. F. Duda, J. F. Lynch, A. E. Newhall, and W. L. Siegmann, "Nonlinear internal wave parameter extraction from SAR images," *156th Meet. Acoust. Soc. Am.,* Miami, (A) *J. Acoust. Soc. Am.* **124**, 2444 (2008).

[35] A. M. Metzler, W. L. Siegmann, R. N. Baer, and M. D. Collins, "Parabolic equation modeling of anistotropic waves in heterogeneous media," *157th Meet. Acoust. Soc. Am.*, Portland, (A) *J. Acoust. Soc. Am.* **125**, 2500 (2009).

[36] S. V. Kaczkowski, W. L. Siegmann, W. M. Carey, A. D. Pierce, and W. Saintval, "Relationships between intrinsic sediment attenuation, modal attenuation, and transmission loss in experiments over sandy-silty sediments," *158th Meet. Acoust. Soc. Am.*, San Antonio, (A) *J. Acoust. Soc. Am.* **126**, 2167 (2009).

REPORT DOCUMENTATION PAGE

Form Approved
OMB No. 0704-0188

1. REPORT DATE *(DD-MM-YYYY)*	2. REPORT TYPE	3. DATES COVERED *(From - To)*
02-26-2010	Final Technical	1 Oct 2003 - 30 Sept 2009

4. TITLE AND SUBTITLE
Shallow Water Propagation

5a. CONTRACT NUMBER

5b. GRANT NUMBER
N00014-04-1-0016

5c. PROGRAM ELEMENT NUMBER

6. AUTHOR(S)
Siegmann, William L

5d. PROJECT NUMBER
09PR00646-00

5e. TASK NUMBER

5f. WORK UNIT NUMBER

7. PERFORMING ORGANIZATION NAME(S) AND ADDRESS(ES)
Rensselaer Polytechnic Institute
110 Eighth Street
Troy, NY 12180-3590

8. PERFORMING ORGANIZATION REPORT NUMBER

9. SPONSORING/MONITORING AGENCY NAME(S) AND ADDRESS(ES)
Office of Naval Research
875 North Randolph Street
Arlington, VA 02210-2109

10. SPONSOR/MONITOR'S ACRONYM(S)
ONR

11. SPONSOR/MONITOR'S REPORT NUMBER(S)

12. DISTRIBUTION/AVAILABILITY STATEMENT
Approved for Public Release; distribution is Unlimited.

13. SUPPLEMENTARY NOTES

14. ABSTRACT
This is the Final Technical Report for ONR Award Number N000140410016. During the performance period, six students received their PhD degrees with ONR support, and their initial and current positions are provided in Section IV. Twenty-one papers were published, and their references are listed in Section V. Thirty-six professional presentations were made, and their titles and venues are given in Section VI. Some research results and figures from the performance period are highlighted in Sections II and III.

15. SUBJECT TERMS
acoustic propagation, shallow water, ocean environmental features, data comparisons, propagation model development

16. SECURITY CLASSIFICATION OF: a. REPORT	b. ABSTRACT	c. THIS PAGE	17. LIMITATION OF ABSTRACT	18. NUMBER OF PAGES	19a. NAME OF RESPONSIBLE PERSON
U			UU	31	William L. Siegmann
					19b. TELEPHONE NUMBER *(Include area code)* (518) 276-6905